Scaling of Vibration Energy Harvester

Kaleb Branda, Tsegereda Esatu, Xiaoer Hu

May 13, 2019

Motivation

- Vibrational energy harvesting become viable alternatives because of the limitations of batteries, along with the reduction of power consumption and size. [1]
- Working frequency range of conventional resonance devices can be increased using nonlinearities obtained through geometrical design. [2]
- As devices continue to shrink, it is also necessary to miniaturize energy harvesters while maximizing power.

Background

- Wideband MEMS energy harvesters
  - Well-suited to extract power from a wide spectrum of vibrations.
  - Greater output power and wide bandwidth due to inclined springs. [3]
- Applications:
  - Bridge or structural constructions wireless monitoring sensors.
  - Wearable and implantable sensors.
  - Automotive tire pressure monitoring systems (TPMSs).

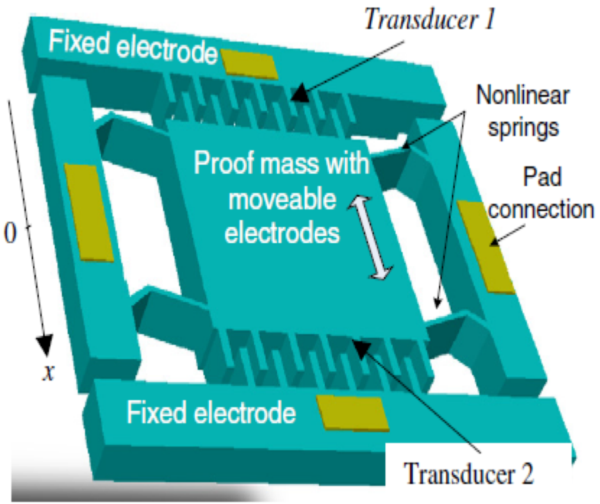

Figure 1. Schematic drawing of a MEMS electrostatic energy harvester with nonlinear springs. [4]

Device Description

- Electrostatic vibrational energy harvester.
- Angled spring to achieve nonlinearities.
- Fabrication: SOI DRIE process with three photolithography masks.

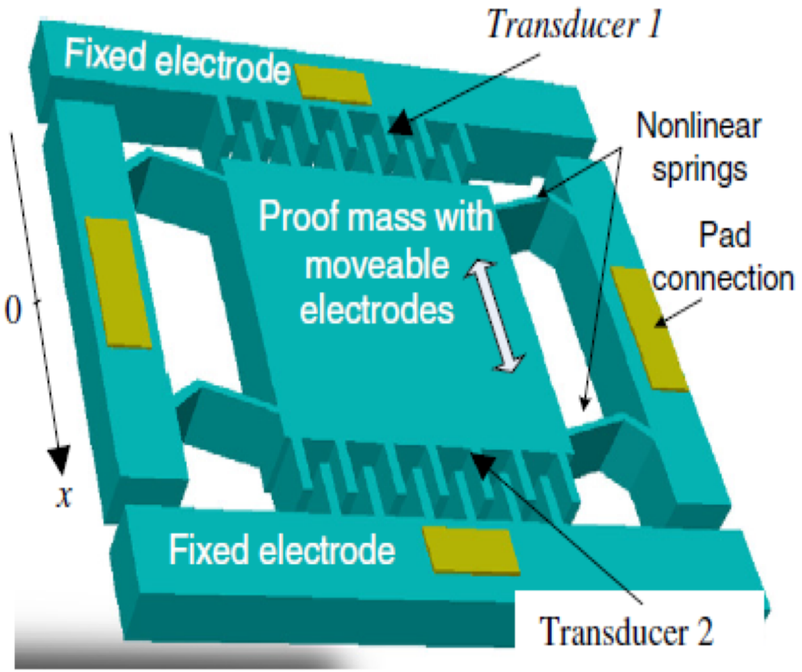

State-of-the-art Vibration Energy Harvesting Devices

Hypothesis: Scaling the vibration energy harvester down will increase power output per mass of the device.

Ref	Year	Specific Power (W/kg)
4	**2010**	**1.22e-2**
5	2011	1.27e-3
6	2013	3.10e-5
7	2013	9.35e-3
Our Scaling Target		>1e-1

Modeling the Harvester with Equivalent Circuit

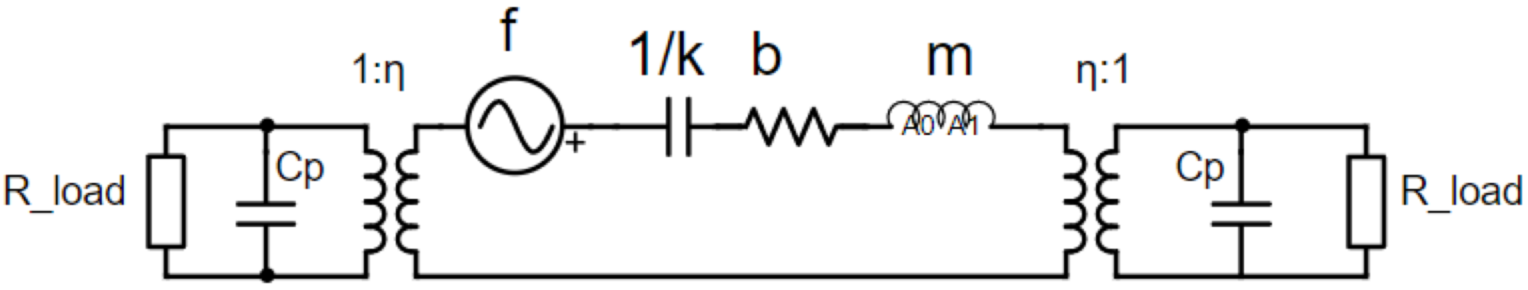

From this we can find the power transferred across both loads as

$$P = 2 \times R_{load} \left[\frac{1}{\sqrt{2}} \cdot \frac{1}{1 + sCR_{load}} \cdot \frac{f\eta}{b + \frac{k}{s} + sm + 2\eta^2 \left(\frac{R_{load}}{1+sCR_{load}} \right)} \right]^2$$

$$\eta = 2N_f V_p \frac{\epsilon_0 h}{g} \qquad R = \frac{b}{\sqrt{4\eta^4 + b^2 C^2 \omega_0^2}}$$

Model with Experimental Results

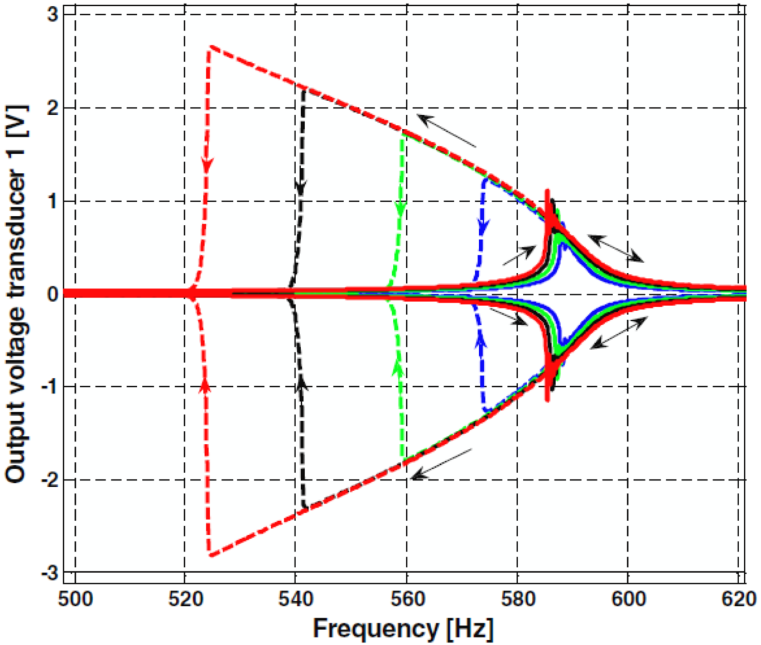

(a)

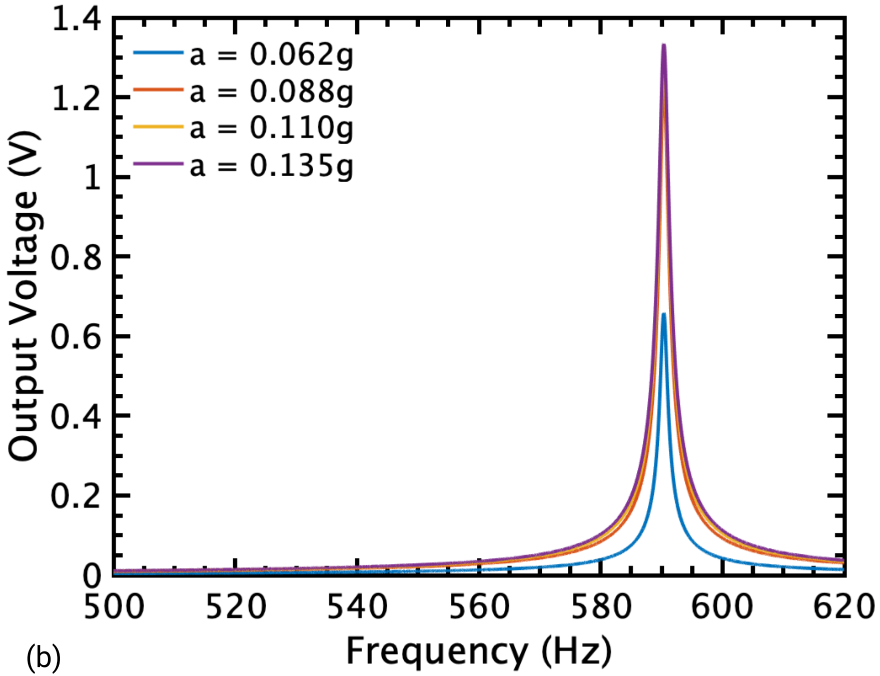

(b)

Figure 2: Peak output voltages as a function of frequency (a) Literature experimental results (b) Generated model.

Model with Experimental Results

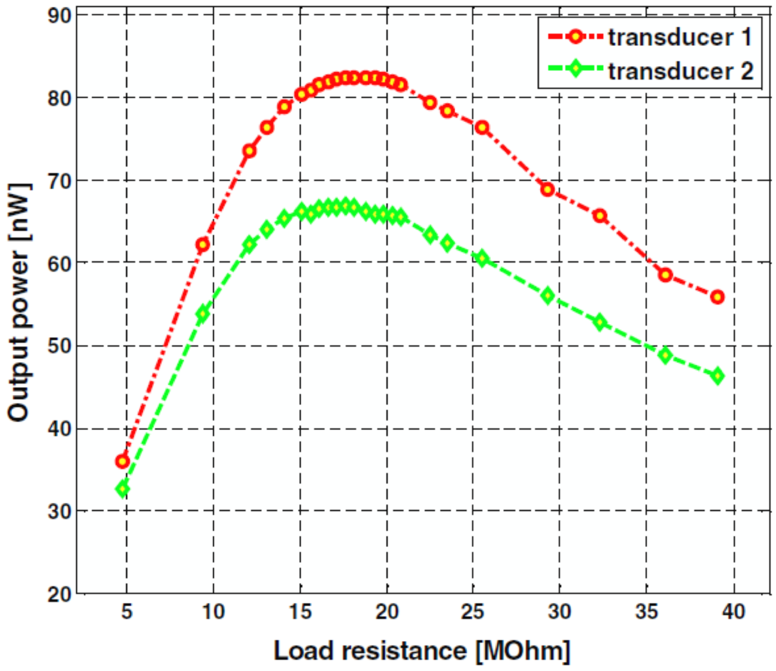

(a)

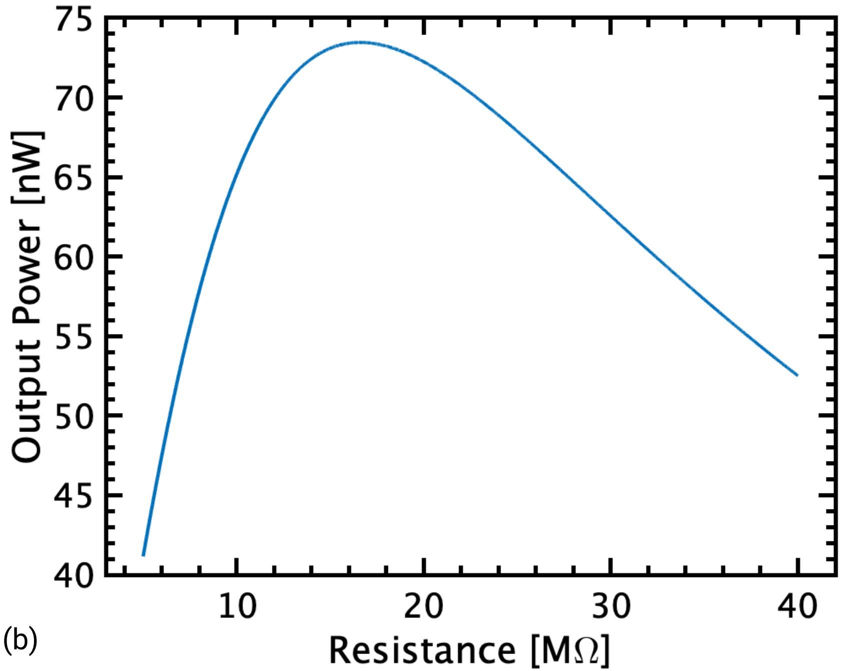

(b)

Figure 3: Output power as a function of load resistance for sinusoidal vibration, with acceleration of 0.14g and a bias voltage of 28.4 V (a) Literature experimental results (b) Generated model.

Two Types of Scaling

$$P = 2 \times R_{load} \left[\frac{1}{\sqrt{2}} \cdot \frac{1}{1 + sCR_{load}} \cdot \frac{f\eta}{b + \frac{k}{s} + sm + 2\eta^2 \left(\frac{R_{load}}{1+sCR_{load}} \right)} \right]^2 \qquad \eta = 2N_f V_p \frac{\epsilon_0 h}{g}$$

- Scaling Finger Gaps
  - Only affects η
  - Equal effect by decreasing the gaps as increasing the number of fingers
  - Does not affect quality factor or resonant frequency significantly
  - Affects load resistance
- Scaling Entire Structure
  - Affects damping, stiffness, mass and gaps
  - Reduces allowed bias voltage (changes η)
  - Shifts resonant frequency but should not change quality factor
  - Affects load resistance

Final Structure Specifications

Description	Original	Gap Scaled (S=7.5)	Fully Scaled (S=1000)
Mass	35.25 mg	35.25 mg	35.25 pg
Thickness	300 μm	300 μm	300 nm
Beam Length	~1400 μm	~1400 μm	1.4 μm
Beam Width	20 μm	20 μm	20 nm
Transducer Gap	15 μm	2 μm	15 nm
Finger width	15 μm	2 μm	15 nm
Initial Capacitive Overlap	~120 μm	~120 μm	120 nm
Number of fingers	128	960	128
Bias Voltage	28.4 V	10.1 V	0.1 V

Model Assumptions for Scaling

- Damping Coefficient
  - Damping from Couette flow dominates

$$b = \mu A / g$$

  - Area scales but undercut of release etch does not
  - Viscous damping from the gaps around the fingers is negligible
- The spring coefficient is near linear in the region of operation
  - k scales with S
- All length dimensions of capacitance scale with S
  - C scales with S

Scaling Finger Gaps

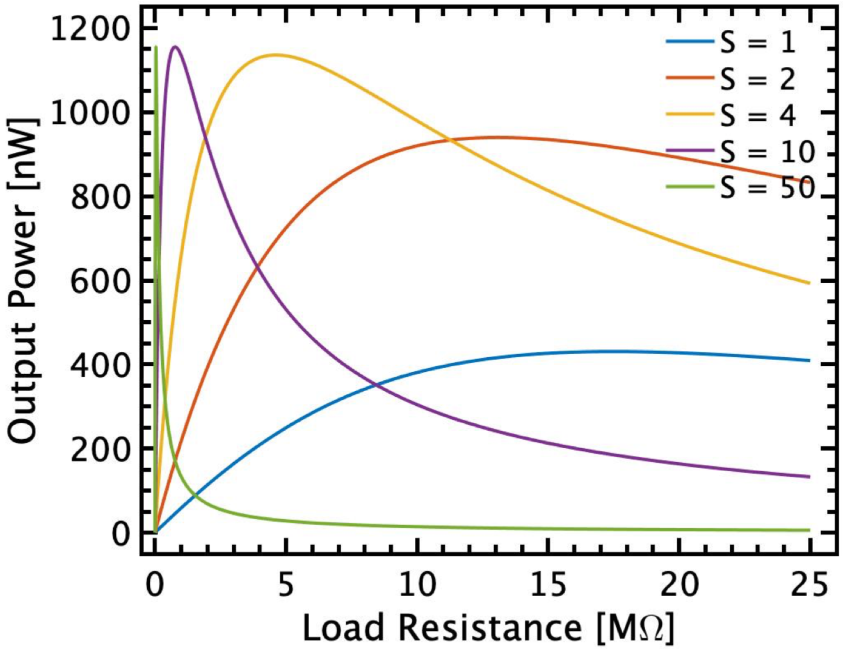

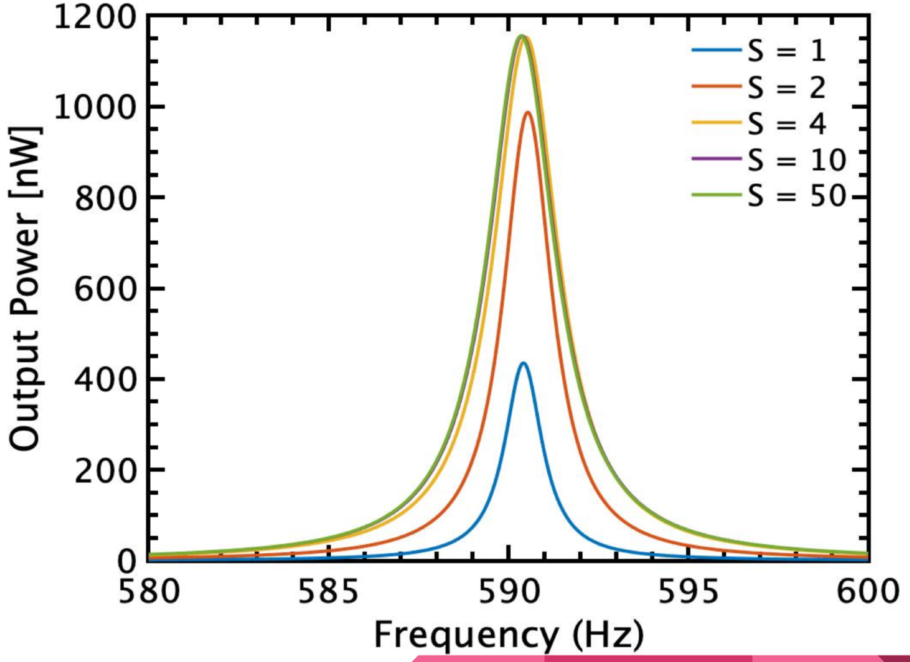

Trend of Scaling Finger Gaps

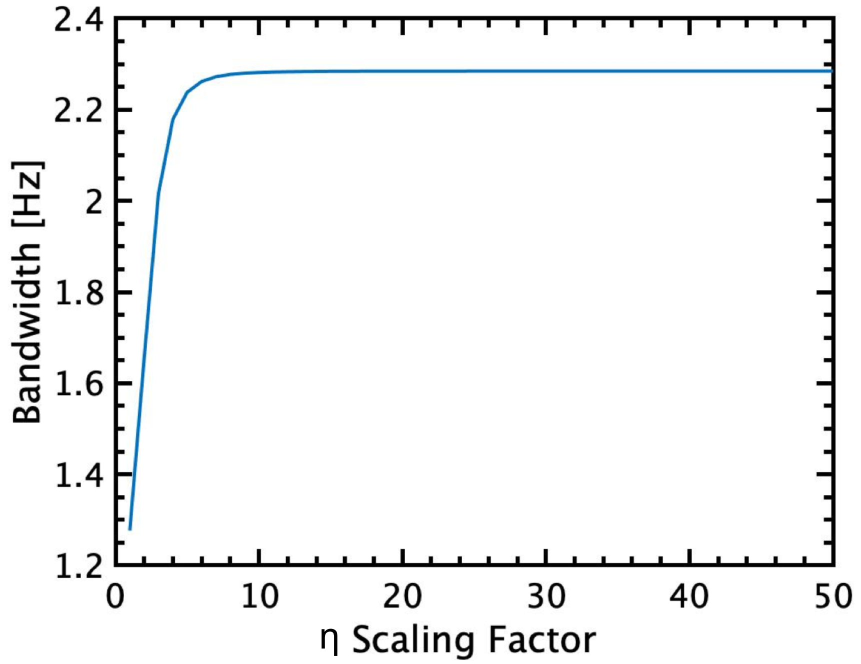

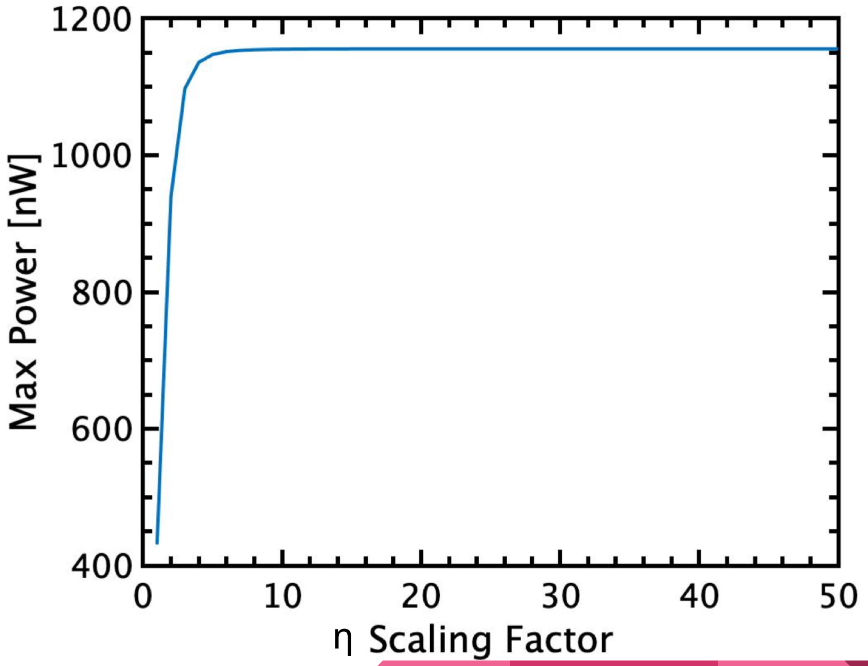

Interpretation

$$P_{resonance} = R\left(\frac{1}{1+sCR}\cdot\frac{f\eta}{b+2\eta^2\left(\frac{R}{1+sCR}\right)}\right)^2 \qquad R = \frac{b}{\sqrt{4\eta^4 + b^2C^2\omega_0^2}}$$

As η increases,

$$R \to \frac{b}{2\eta^2}, \qquad \frac{1}{1+sCR} \to 1, \qquad P_{resonance} \to \frac{f^2}{8b}$$

Physical interpretation:

- The resistive load dominates the output impedance
- The increased coupling decreases optimal load and counteracts increase in current

Scaling the Entire Structure 1000x

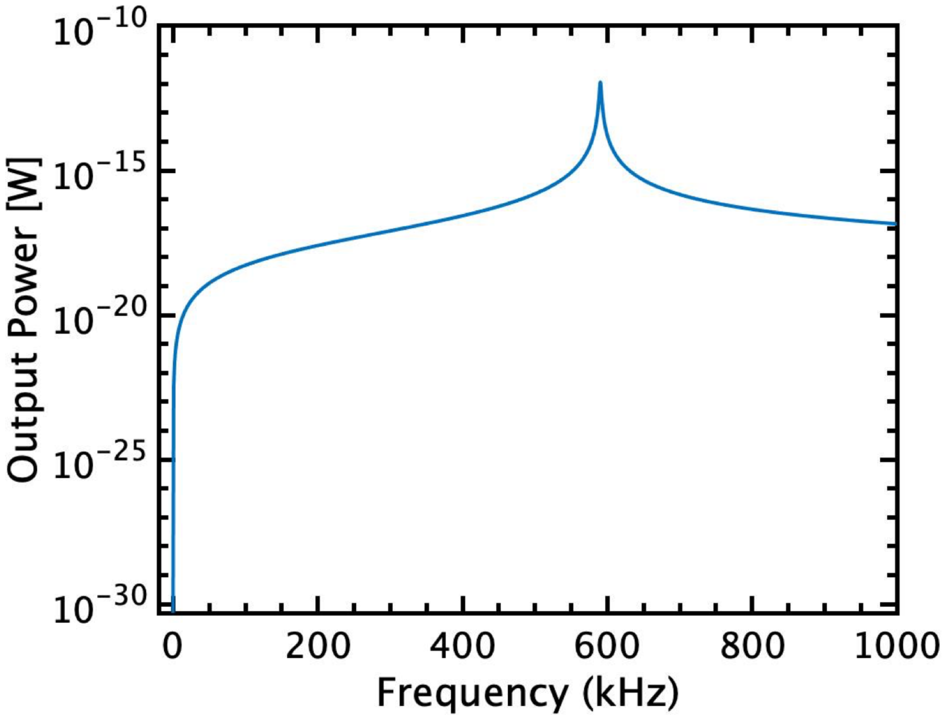

Trend of Scaling the Entire Structure

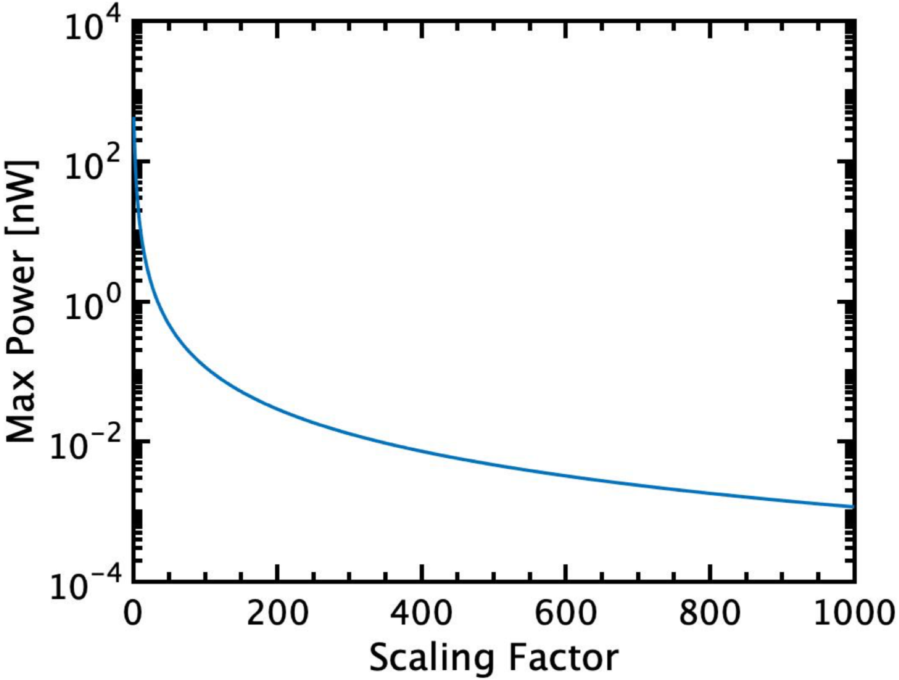

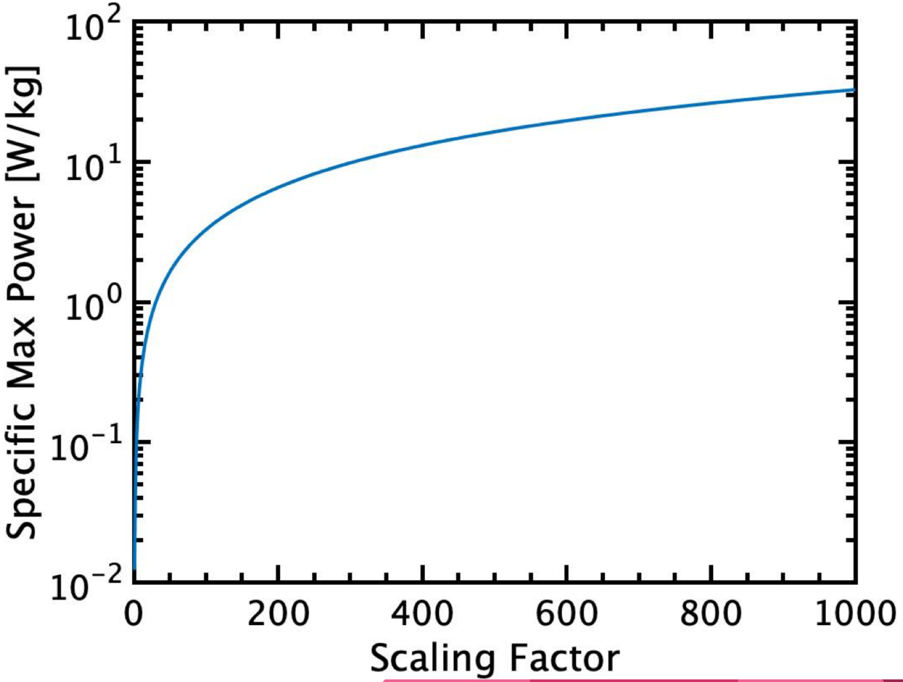

Final Structure Specifications

Description	Original	Gap Scaled (S=7.5)	Fully Scaled (S=1000)
Mass	35.25 mg	35.25 mg	35.25 pg
Thickness	300 µm	300 µm	300 nm
Beam Length	~1400 µm	~1400 µm	1.4 µm
Beam Width	20 µm	20 µm	20 nm
Transducer Gap	15 µm	2 µm	15 nm
Finger width	15 µm	2 µm	15 nm
Initial Capacitive Overlap	~120 µm	~120 µm	120 nm
Number of fingers	128	960	128
Bias Voltage	28.4 V	10.1 V	0.1 V

Conclusion

	Original	Gap Scaled (S=7.5)	Fully Scaled (S=1000)
Power output (per mass)	0.16 W/kg	0.74 W/kg	7.37 kW/kg
Resonant Frequency	590 Hz	590 Hz	590 kHz
Bandwidth (FWHM)	1.28 Hz	2.28 Hz	2284.6 Hz
Peak specific power output (per mass)	0.0122 W/kg	0.033 W/kg	32.78 W/kg
Load Resistance	17.5 MΩ	0.19 MΩ	76.4 kΩ

Scaling down the device:

- Increases output power per mass
- Raises resonance frequency
  - Problem for spectrums with low frequency
- Decreases needed bias voltage
- Drives low load resistance
- Increases bandwidth

References

[1] Boisseau, S et al. "Optimization of an electret-based energy harvester." *Smart Materials and Structures* 19.7 (2010): 075015.

[2]Y. Suzuki, D. Miki, M. Edamoto, and M. Honzumi, “A mems electret generator with electrostatic levitation for vibration-driven energy harvesting applications,” J. Micromech. Microeng., vol. 20, no. 10, p. 104002, 2010

[3] L. G. W. Tvedt, S. D. Nguyen, and E. Halvorsen, ”Nonlinear behavior of an electrostatic energy harvester under wide- and narrowband excitation,” IEEE/ASME Journal of Microelectromechanical Systems, vol. 19, no. 2, pp. 305-316, Apr 2010.

[4] Nguyen, D. S., et al. "Fabrication and characterization of a wideband MEMS energy harvester utilizing nonlinear springs." *Journal of Micromechanics and Microengineering* 20.12 (2010): 125009.

[5] Cepnik, C and Wallrabe, U. 2011. A Micro Energy Harvester with 3D Wire Bonded Microcoils. (Beijing, China: IEEE, Transducers’11) pp 665–8

[6] Ju S, Chae S H, Choi Y, Park S M, Lee S, Lee H W and Ji C-H. 2013. Frequency up-converted low frequency vibration energy harvester using trampoline effect Power. *MEMS J. Phys.: Conf.* Ser. 476 012089

[7] Choi Y, Ju S, Chae S H, Jun S, Park S M, Lee S, Lee H W and Ji C-H. 2013. Low frequency vibration energy harvester using a spherical permanent magnet with non-uniform mass distribution. *Power MEMS J. Phys.: Conf.* Ser. 476 01212